Slag physical property models and data: A review of structure, viscosity, electrical conductivity, and thermal conductivity

H. Muire[1,2], S. Zaaiman[1,2], and J.H. Zietsman[1,2]

[1]Ex Mente Technologies, South Africa
[2]University of Pretoria, South Africa

Computational modelling can help us in the pyrometallurgical industry to increase our understanding of our materials and processes, improve our existing operations, and develop new production technologies. These activities are critical, given the growing challenges of energy availability, raw material quality, and environmental pressure. Importantly, modelling can enable us to do these things faster, with less uncertainty, and with much less risk. Our ability to accurately determine slag structure and calculate slag physical properties such as viscosity, electrical conductivity, and thermal conductivity is, however, limited to how well we can describe high-temperature processes with computational models. Extensive collections of measured physical property data for slag systems can be found in the 1995 2nd Edition of the Slag Atlas. In addition, Professor Ken Mills presented a short course on slag models at the SAIMM Pyrometallurgy Conference in 2011 and made available an excellent handbook and spreadsheet for making calculations. These data and models are used to estimate slag physical properties at different temperatures and compositions. Since the Slag Atlas and the short course by Professor Mills, more property data have been generated with new and improved measurement and computational methods, and improved property models have been developed. There is, therefore, an opportunity to review the literature to create updated collections of property data and models for describing slag physical properties. In this paper, we review the current state of data and models for estimating the structure, viscosity, electrical conductivity, and thermal conductivity of liquid slags. We present this work to increase awareness of the importance of the physical properties of slag models to our industry, and to provide our community with up-to-date resources for calculating some of these properties as part of practical applications. The work is a step towards a comprehensive collection of updated reviews and resources relating to the physical properties of slags.

INTRODUCTION

Slag behaviour and properties are important aspects of pyrometallurgical processes to effectively extract alloys from metal ores. The smelting of metal ores produces a liquid alloy and slag. In this review we use the term 'slag' specifically to refer to a liquid solution that consists of metal and metalloid oxides. It contains the oxides that are reduced to metals in reduction processes and can serve to seal off alloy and matte baths from oxygen and extract undesirable elements from the alloy (Mills, 2011).

By understanding the structure and properties of slag, we can gain insight into the behaviour of a process. Physical property models and data can be used to achieve this objective. However, providing a comprehensive repository of slag physical property data and models is daunting, given the large number of slag systems and the different properties that need to be described.

Therefore, the work presented here is a first iteration and focuses only on high-TiO_2 and ferrochrome slags. Slag structure, viscosity (μ), electrical conductivity (σ), and thermal conductivity (κ) are the only properties considered with models and data reported on post-publication of the Slag Atlas (Allibert and Verein Deutscher Eisenhüttenleute, 1995).

Mills (2011) explained that there are various model types to calculate slag physical properties, including (1) numerical fits, (2) neural network models, (3) models based on structural parameters, (4) thermodynamic models, and (5) molecular dynamics (MD) models. In this review, we focus on models using structural parameters that are incorporated into Arrhenius-type relations.

The Arrhenius equation, Equation 1, was originally formulated to describe the temperature dependence of the rate constant (k) for chemical reactions.

$$k = Ae^{\frac{-E_a}{RT}} \quad [1]$$

It also found application in describing the temperature dependence of material physical properties. Therefore, the term Arrhenius-type relations in the context of this review refers to relations based on the Arrhenius or related equations, such as Equation 4 and Equation 5. These semi-empirical models are parameterised with activation energy E_a and pre-exponential factor A, which are commonly expanded into more terms to incorporate slag structure through additional temperature and compositional dependencies.

Other model types are only briefly mentioned when the reviewed literature referred to them. For insight into structure-based thermodynamic models the reader is recommended to review literature on the associated solution model, cell model, modified quasichemical model, and sub-lattice model applied to slag systems (Allibert and Verein Deutscher Eisenhüttenleute, 1995). MD models are discussed by Zaaiman, Muire, and Zietsman (2024).

The Slag Physical Properties section provides an overview of each property that is not slag specific. Physical property models for high-slags are discussed in the High-TiO_2 Slag Property Models section and for ferrochrome slags in the Ferrochrome Slag Property Models Section. Finally, the Slag Physical Property Data Section provides references where data for the two slag systems can be found.

Slag Physical Properties

This section presents an overview of the investigated slag physical properties to provide some important necessary background. Slag structure is addressed first, as it influences all the other physical properties. μ, σ, and κ are then considered.

Structure

Slag composition and temperature are the main factors that determine structure and consequently physical properties. This is exhibited by the silicate network structure found in many slags. Slag in a liquid state, inferring a high temperature, with composition proportionally high in SiO_2 forms a network type structure (Mills *et al*., 2011). Changes in temperature or composition, such as the SiO_2 content, influence this structure and the resulting physical properties.

Constituent Ions

A slag is a mixture of ions that include oxygen anions O_2^- , metal cations M^{n+}, silicate anions (e.g. SiO_4^{4-}), and ions from non-metal oxides such as P_2O_5 and SO_3. Two bond types exist in a slag, namely (1) covalent Si-O-Si bonds that form structures such as chains and rings, and (2) ionic bonds that involve cations such as Na^{2+} or Ca^{2+} (Si-O-Na or Si-O-Ca) that impede or break the formation of a silicate network (Mills *et al.,* 2011).

Figure 1a shows that a silicate structural unit is a tetrahedron that consists of Si^{4+} ion surrounded by four O^{2-} ions. An O^{2-} ion's two electrons can bond (1) to Si^{4+} cations or (2) to cations such as Na^{2+} and Ca^{2+}. Oxygen ions are classified as follows:

- **Bridging oxygens** (BO or O^0): Both electrons are bonded to ions, forming a *'bridge'* between the two cations. These anions build silicate networks.
- **Non-bridging oxygens** (NBO or O^-): One electron is bonded to an Si^{4+} ion, and the second to another cation, e.g. Ca^{2+}. These O_2^- anions break silicate networks.
- **Free oxygens** (O_2^-): Neither electron is bonded to an ion or any other ion.

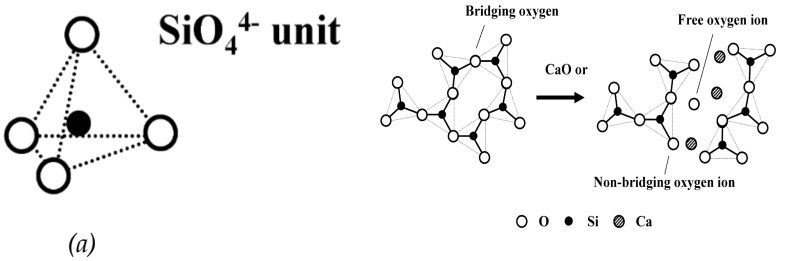

(a) *(b)*

Figure 1. Silicate slag structure (Nakamoto et al.*, 2007), © 2024 The Iron and Steel Institute of Japan.*

Constituent Compounds
Slag constituent compounds are classified as follows:

- **Network formers** or **acidic oxides**: Oxides that promote the formation of network structures, e.g. SiO_2.
- **Network breakers** or **basic oxides**: Oxides that terminate and break network structures, e.g. CaO, Na_2O.
- **Amphoteric oxides**: Al_2O_3 is an example. It contributes Al^{3+} ions that can be absorbed into Si^{4+} chains. This requires charge-balancing cations such as Na^+ or 0.5 Ca^{2+} in proximity to Al^{3+} ions to form, for example, $(NaAl)^{4+}$ ions. Charge-balancing cations cannot act as network breakers (Mills *et al.*, 2011). Al_2O_3 therefore acts as a network former, but in high concentrations Al^{3+} ions can also act as network breakers (Mills *et a*l., 2012). For this reason Al_2O_3 is classified as amphoteric.

Structure Quantification
NBO/T, the ratio of non-bridging oxygens to tetragonal ions is the parameter that is used most widely to quantitatively describe silicate slag structure; see Equation 2. It is a measure of depolymerisation and uses mole fractions of oxygen ions associated with different slag constituents. Constituent mole fractions are represented with x and f which indicates the fraction of M_2O_3 acting as a network breaker. Examples of constituents are MO = CaO, FeO, M_2O = Na_2O and M_2O_3 = Fe_2O_3, Cr_2O_3 (Mills *et al.*, 2012).

$$\frac{\mathrm{NBO}}{\mathrm{T}} = \frac{2\left(x_{\mathrm{MO}} + x_{\mathrm{M_2O}} + 3f x_{\mathrm{M_2O_3}} - x_{\mathrm{Al_2O_3}} - (1-f)x_{\mathrm{M_2O_3}}\right)}{\left(x_{\mathrm{SiO2}} + 2x_{\mathrm{Al_2O_3}} + 2(1-f)x_{\mathrm{M_2O_3}}\right)} \quad [2]$$

Q, degree of polymerisation is another approach to quantify slag structure. It is calculated with Equation 3 and can be expressed in terms of mole fractions of Q^n for the types of silicates with n indicating the number of bridging oxygens per atom (Q^0, Q^1, Q^2, Q^3, Q^4). Expressing Q in terms of Q^n requires additional calculation from an analytical technique, such as Raman spectroscopy, or a structural model describing slag structure. The reader is recommended to review the referenced literature for more information on Q^n (Mills *et al.*, 2011; Mills *et al.*, 2012; Thibodeau *et al.*, 2016).

$$Q = 4 - \frac{\mathrm{NBO}}{\mathrm{T}} \quad [3]$$

NBO/T and Q cannot differentiate between the effects that different cations such as Na^+ or Ca^+ have on slag structure. For this reason the concept of optical basicity (Λ) was developed. It was further improved with corrected optical basicity (Λ^{corr}) to differentiate between cations involved in charge-balancing. Equations for Λ and Λ^{corr} have been omitted from this review due to their extensive length and variation in expression for different slags. Descriptions for Λ and Λ^{corr} can be viewed at the referenced literature (Zhang and Chou, 2010; Mills, 2011; Mills *et al.*, 2012).

Viscosity

At the molecular level, viscosity (μ) describes the extent to which the relative motion of adjacent liquid layers of atoms and molecules are retarded, and can be regarded as a measure of internal friction of the liquid.

Slag viscosity is dependent on structure and ionic mobility, which are determined by composition and temperature. The more polymerised a slag, the higher its viscosity will be.

- **Temperature**: Slag viscosity decreases with increasing temperature. This is due to improved ionic mobility, and because networks can break up as temperature increases.
- **Composition**: Network forming oxides increase slag viscosity, and network breakers decrease it. This is due to silicate networks being more rigid than separate metal cations and oxygen anions.

The temperature dependence of viscosity is commonly described with the Arrhenius equation, Equation 4, or the Weymann-Frenkel equation, Equation 5. The composition dependence is described through the A and E_a parameters (Gan, *et al.*, 2016; Forsbacka *et al.*, 2009).

$$\mu(\mathbf{x}, T) = A(\mathbf{x}, T)e^{\frac{-E_a(\mathbf{x})}{\mathrm{R}T}} \quad [4]$$

$$\mu(\mathbf{x}, T) = A(\mathbf{x}, T)Te^{\frac{-E_a(\mathbf{x})}{\mathrm{R}T}} \quad [5]$$

The most common methods to describe composition dependence are with the Riboud, Urbain, and Iida models. Both the Riboud and Urbain models are based on the Weymann relation and the Iida model is based on the Arrhenius relation (Mills *et al.*, 2011; Mills, 2011; Yan *et al.*, 2021). The Riboud model classifies the slag components into five different categories, depending on their chemical nature and assigns parameters to these categories. The Urbain model classifies slag constituents as glass formers, breakers, and amphoterics; the Iida model makes use of a modified basicity index to describe the network structure of a slag (Seetharaman *et al.*, 2004; Mills *et al.*, 2011; Yan *et al*, 2021).

Further information about slag viscosity models are available in (Mills, 2011; Seetharaman *et al.*, 2004; Mills *et al.*, 2011; Mills *et al.*, 2012; Mills *et a*l., 2013; Gan *et al.*, 2016).

Electrical Conductivity

Electrical conductivity σ is a material's ability to conduct an electrical current. Equation 6 shows that it is determined by two mechanisms, namely ionic conduction and electronic conduction. Electrical resistivity ρ is the inverse of σ.

$$\sigma = \sigma_{\text{ionic}} + \sigma_{\text{electronic}} = \frac{1}{\rho} \quad [6]$$

σ is influenced by both composition and temperature. The Arrhenius equation, Equation 7, is used (Mills *et al*, 2011; Mills *et al.*, 2012; Mills, 2011; Liu *et al.*, 2014; Liu *et al.*, 2016; Liu *et al*, 2017; Liu *et al.*, 2018).

$$\sigma(\mathbf{x}, T) = A(\mathbf{x}, T)e^{\frac{-E_a(\mathbf{x})}{\mathrm{R}T}} \quad [7]$$

The slag systems investigated by Liu *et al.*, (2017) revealed that both σ_{ionic} and $\sigma_{\text{electronic}}$ increase with increasing temperature. All the studied slags follow the Arrhenius relation.

Ionic Conduction
Ionic conduction is the transfer of electrical charge through the movement of individual ions when subjected to an electric field. In slags, the cations (Ca^{2+}, Mg^{2+}, Mn^{2+}, Pb^{2+}, Al^{3+}, and Si^{4+}) are assumed to be the charge carriers for ionic conduction and are supported by rigorous analysis of conductivity results (Bockris *et al.*, 1952a; Bockris *et al.*, 1952b; Thibodeau, 2016).

The partial ionic conductivity contribution ($\sigma_{\text{ionic,i}}$) for cation i in the slag is calculated with Equation 8.

$$\sigma_{\text{ionic,i}} = c_{\text{i}} z_{\text{i}} \text{F} \mu_{\text{i}} \quad [8]$$

σ_{ionic} is the sum of the partial ionic conductivities of all the charge carriers, Equation 9 (Thibodeau, 2016).

$$\sigma_{\text{ionic}} = \sum_{i=\text{cation}} \sigma_{\text{ionic,i}} \quad [9]$$

Electronic Conduction
Electronic conduction is the transfer of electrical charge by the movement of electrons from one atom to an adjacent atom under the influence of an electric field (Mills *et al.,* 2011; Mills *et al.,* 2012; Thibodeau, 2016; Liu *et al.,* 2016).

The $\sigma_{\text{electronic}}$ contribution to σ of a slag system is considered negligible when transition metals, such as Ti, Cr, Mn, and Fe are not present in a slag. However, due to the significant presence of Ti and Cr in high-TiO_2 and ferrochrome slags, to be discussed, the $\sigma_{\text{electronic}}$ contribution to the σ is not negligible and must be considered for these slags (Thibodeau, 2016).

Thermal Conductivity
Thermal conductivity κ is a material's ability to transfer heat through conduction. It is influenced by composition and temperature. κ is influenced by mechanisms of phonon thermal conduction, thermal radiative conduction, and electronic thermal conduction. All these contributions should be considered, Equation 10, when calculating a material's κ as they can have a considerable effect on the final material property value (Allibert. and Verein Deutscher Eisenhüttenleute, 1995).

$$\kappa = \kappa_{\text{phonon}} + \kappa_{\text{radiative}} + \kappa_{\text{electronic}} \quad [10]$$

Phonon Thermal Conduction
Phonon thermal conduction is the transfer of heat through a medium by phonons (lattice waves) and is associated with the vibrational modes of molecules within a sample. It is also referred to as lattice conduction. The scattering of phonons causes a decrease in the thermal conductivity of a material and can occur by collisions with other phonons, grain boundaries or crystal imperfections (Allibert and Verein Deutscher Eisenhüttenleute, 1995).

Phonon conduction is structure-dependent and for liquid slags it is represented by Equation 11 (Mills and Susa, 1992).

$$\kappa_{\text{phonon}} = \frac{1}{3}\left(C_p \cdot v \cdot l\right) \quad [11]$$

Phonons travel along the crystal lattice for a solid and for slags; the route of travel for phonons is provided by the network (Kotzé, 2020). A higher degree of polymerisation therefore causes higher κ_{phonon}.

Radiative Thermal Conduction
Radiative thermal conduction is a mechanism by which radiant heat is transferred through sections of a medium with the absorption and emittance of photons. A thin section of slag absorbing radiant heat or photons will increase in temperature and emit photons again to cooler sections. This can occur continuously through a medium and the energy transferred will increase as the absorption and emittance of photons progress through additional sections until $\kappa_{\text{radiative}}$ reaches a constant value. The

slag is then termed optically thick; this is considered to occur when the combined term of the absorption coefficient (a) and the thickness of the sample (d) is $ad > 3.5$ (Allibert and Verein Deutscher Eisenhüttenleute, 1995).

The $\kappa_{\text{radiative}}$ for optically thick samples, with assumptions of steady-state and grey-body conditions, can be calculated with Equation 12.

$$\kappa_{\text{radiative}} = \frac{16\sigma n^2 T^3}{3a} \quad [12]$$

For optically thin samples ($ad < 3.5$), Equation 13 and 14 can be used to calculate $\kappa_{\text{radiative}}$ with tabulated data for the reflection coefficient of the boundary, ($R = 1 - \epsilon$) (Allibert and Verein Deutscher Eisenhüttenleute, 1995).

$$\kappa_{\text{radiative}} = 8n^2\sigma T^3 \left\{ \frac{(1-R)}{2(1+R)} - \frac{\tau(1-4R+R^2)}{(1+R)^2} \right\} \quad [13]$$

$$\kappa_{\text{radiative}} = \frac{16n^2\sigma T^3}{3} f(\epsilon, \tau) \quad [14]$$

Electronic Thermal Conduction
Electronic thermal conduction is the transfer of heat through a medium by electrons and is associated with the electronic structure of a sample (Allibert and Verein Deutscher Eisenhüttenleute, 1995).

Similar to $\sigma_{\text{electronic}}$ contribution not being negligible towards slag σ with significant transition metal cation contents, the $\kappa_{\text{electronic}}$ contribution may also be significant and should be factored in when calculating κ.

High-TiO_2 Slag Property Models

Physical property models specific to high-TiO_2 slags are described in this section. Slag composition is first explained, followed by a structural description. Arrhenius-type models are then discussed for viscosity, electrical conductivity, and thermal conductivity.

Composition

TiO_2-rich slag is produced through the smelting of ilmenite ($FeTiO_3$). The main impurities are MnO, MgO, SiO_2, and Al_2O_3 which amount to about 3% of the mass of ilmenite. These slags have compositions close to pseudobrookite stoichiometry (M_3O_5) and can be viewed as a mixture of Ti_3O_5 , $FeTi_2O_5$, $MnTi_2O_5$, Al_2TiO_5 , $MgTi_2O_5$, V_2TiO_5, and Cr_2TiO_5 (Pistorius, 2008; Zietsman and Pistorius, 2004).

Titania slag compositions are commonly expressed in terms of TiO_2 content, because analytical methods measuring total titanium content are fast and less cumbersome than wet chemical titration required to distinguish between Ti^{3+} and Ti^{4+} (Kotzé, 2020). If a significant amount of Ti_2O_3 is included in the TiO_2 value; titania content is expressed as an equivalent TiO_2 (TiO_{2eq}), with all Ti expressed as TiO_2.

The TiO_2 content limit for what can be considered a high-TiO_2 slag is unclear. For the industrial process in making TiO_2 pigment involves a chlorination step that requires a high-slag feedstock with TiO_2> 85% (Pistorius, 2008). The viscosity work of Hu *et al.*, (2021) considered titania slags with TiO_2 > 70 mass%. In this paper a slag is considered high-titania if the TiO_2 content is greater than 70 mass%.

Structures

Unlike silicate slags, the structure of high-TiO_2 slags is not well understood. Handfield and Charette (1971) explain that none of the ionic theories, originally developed for silicate slags, can be applied to satisfactorily describe the structure of high-TiO_2 slags. TiO_2 slags consist of mostly, Ti^{3+}, Ti^{4+}, and Fe^{2+} cations, and their structure is not comparable to silicate slags that contain SiO_2 networks (Pesl and Hurman, 1999; Kotzé, 2020; Hu *et al.,* 2021). Consequently the viscosity of high-TiO_2 slags is very low.

There is a relation between the coordination numbers of metal atoms in a slag and its viscosity (Handfield and Charette, 1971). High cation coordination numbers of six and more have low viscosities and lower coordination numbers of four and less have high viscosities. The average Ti^{4+} coordination number in titanosilicate melts increases with concentration (Mysen and Richet, 2019). This reveals a relation between content, slag structure (Ti^{4+} coordination numbers), and slag viscosity.

Further work is required to develop a structural description for high-TiO_2 slags and its relation to the viscosity. MD work has shown interesting structural information for these slags. Ti is found to be six-coordinated with O and indicates that Ti^{4+} tends to form a three-dimensional TiO_6 octahedral network structure in the slag (Hu *et al.*, 2018; Kim and Park, 2019).

Viscosity

The incomplete structural description of high-TiO_2 slags results in limited viscosity models being available for these slags. Experimentally measured viscosities are very low, in the range of 0.15 dPa s to 1 dPa s, and it is not sensitive to composition and temperature changes above the liquidus temperature (Handfield and Charette, 1971; Kotzé, 2020; Hu *et al.*, 2018; Hu *et al.*, 2021).

Only in recent studies have models for estimating the viscosity of high-TiO_2 slags been developed. Hu *et al.*, (2021) mentioned that there was no suitable model yet to describe high-TiO_2 slags and set about developing one. The model developed is based on the Vogel-Fulcher-Tammann (VFT) semi-empirical formalism that has previously been used to describe the viscosity of glasses. To provide an adequate description of the aggressive crystallisation and sensitivity to temperature for high-TiO_2 slags near the liquidus temperature, (see Figure 2), the viscosity-composition-temperature relationships had to be factored in correctly.

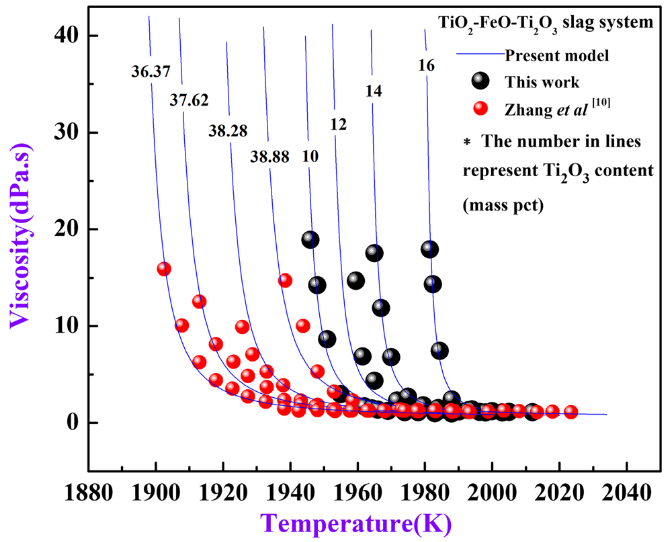

Figure 2. Estimated viscosity of TiO_2–FeO–Ti_2O_3 system with experimental results (Hu et al. *2021), © CC BY 4.0.*

Therefore, the parameters B and C in the VFT equation, Equation 15, were made composition-and temperature-dependent.

$$\log \mu(\mathbf{x},T) = \log \mu_{\infty}(x) + \frac{A(\mathbf{x},T)}{T - T_0(\mathbf{x},T)} = A + \frac{B}{T - C} \quad [15]$$

Parameter A, Equation 16, is composition-dependent only and is the value of $\log(\mu(x))$ (Pa s) at infinitely high temperature. C denotes the temperature (K) at which viscosity becomes infinite and parameter B corresponds to the pseudo-activation energy associated with viscous flow. It is thought to represent a potential energy barrier obstructing the structural rearrangement of the slag. Both B and C, Equation 17

and 18, are related to temperature by considering a linear relationship and to slag composition by considering binary interactions between each component (Hu *et al.*, 2021).

$$A = \log \mu_{\infty}(x) = \sum_{i=1}^{n} r_i \, x_i \quad [16]$$

$$B = A(T, x) = \sum_{i=1}^{n} \sum_{j=1}^{m} \left[x_i x_j \left(a_{ij} + b_{ij} T \right) \right] \quad [17]$$

$$C = T_0(T, x) = \sum_{i=1}^{n} \sum_{j=1}^{m} \left[x_i x_j \left(c_{ij} + d_{ij} T \right) \right] \quad [18]$$

where $i \neq j, a_{ij}, b_{ij}, c_{ij} = a_{ji}, b_{ji}, c_{ji}$, and $b_{ii} = b_{jj} = d_{ii} = d_{jj} = 0$, x_i or x_j are component molar fractions and $r_i, a_{ij}, b_{ij}, c_{ij}, d_{ij}$ are fitting parameters. Optimised parameters can be found in the source literature (Hu *et al.* 2021)

The study concluded that high-TiO_2 slags have a very low viscosity of around 0.8 dPa s that exhibits a negligible dependence on the temperature and composition even with an additional increase in temperature. The proposed model is capable of estimating the viscosities of the TiO_2–FeO–Ti_2O_3 system over wide molar composition ranges; TiO_2: 0.598–0.890, FeO: 0.027–0.954, and Ti_2O_3: 0.058–0.375 and a temperature range of 1663 K to 2020 K. The average relative error for this model is 18.82%.

Electrical Conductivity

The review study of Yan *et al.*, (2021) reveals that most high-TiO_2 slags yield high electrical conductivity above the liquidus temperature and that electronic conduction is predominate over ionic conduction. The theoretical mechanism of "small polaron hopping", proposed by Mott (1968), for electronic conduction in transition metal oxide glasses was postulated to also apply to high-TiO_2 slags (Yan *et al.*, 2021; Hu *et al.,* 2019; Liu *et al.,* 2016). The mechanism is described as conduction performed by electrons jumping, through thermal excitation of heat transfer, from low valence cations to adjacent high valence transition metal cations. Both low-valence and high-valence cations are required for this mechanism to function.

With regards to the high-TiO_2 slag, it is described as a random walk of electrons between tetravalent titanium and trivalent titanium dispersed in the melt with polaron hopping being the driving influence (Hu *et al.*, 2019).

Hu *et al.* (2019) re-iterates that the ionic conductivities resulting from Ca^{2+}, Mg^{2+}, Ti^{4+}, Ti^{3+} and Fe^{2+} is always present in a slag. In a fully liquid state, it is reasonable to speculate that the electrical conductivity of high- slag is an electronic-ionic mixed conductivity, with electronic conduction being the dominating effect.

Yan *et al.,* (2021) references there are electrical conductivity models based on Arrhenius-type relations for silicate slags in the ionic conduction range but none exist for high-TiO_2 slags that require the effect of electronic conduction to be incorporated.

A correlation using Equations 19 to 21 based on Desrosiers *et al.*, (1980) experimental electrical conductivity data is currently the only model available for estimating the electrical conductivity of high-TiO_2 slags (Kotzé, 2020). It uses the polarisability of the oxide components, Table 4 in reference, in the slag to estimate the electrical conductivity.

$$\sigma = b \left(\frac{\beta_{slag}}{10} \right)^m \quad [19]$$

$$\beta_{slag} = \sum_{i=1}^{n} X_i \, \beta_i \quad [20]$$

$$R_{\text{valency}} = \frac{X_{\text{Fe}^{2+}} + X_{\text{Ti}^{3+}}}{X_{\text{Fe}^{2+}} + X_{\text{Ti}^{3+}} + X_{\text{Ti}^{4+}}} \quad [21]$$

For reported high-gangue slag, Equations 19 and 20 produce estimations that are in good agreement with the experimental measurements. The addition of Equation 21, a temperature-dependent valency ratio, to Equation 19 is required for low-gangue slag to improve the estimation towards measured electrical conductivity values (Kotzé, 2020; Desrosiers *et al*., 1980). No relative errors are provided and Kotzé, (2020) reported that the model applied to example industrial titania slags in the study could not be verified as there were no experimental electrical conductivity measurements for these slags.

Thermal Conductivity

The study of Heimo *et al*., (2019), described that there is a lack of thermal conductivity values for high-slags, especially as a function of temperature. Experimental measurements for the thermal conductivity were produced from the study but no model for the property. The review of literature eventually only revealed one model to adequately describe the thermal conductivity of liquid high-TiO_2 slag.

In the study of Kotzé, (2020), thermal conductivity values for a set of high-TiO_2 slags were estimated with Equations 11, 12 and 22 at 1650, 1700, and 1750 K. The model results were only graphically represented and there is no experimental data to verify the estimated values. The $\kappa_{\text{electronic}}$ contribution was calculated with the Wiedemann-Franz formula, Equation 22, that utilises determined σ values; the Lorenz number (L) and a specific temperature (T) in K (Kotzé, 2020; Ok *et al*., 2018).

$$\kappa_{\text{electronic}} = \sigma L T \quad [22]$$

Ferrochrome Slag Property Models

This section describes physical property models specific to ferrochrome slags. The composition is first defined for ferrochrome slag systems and then the structure is discussed. This is followed by descriptions of Arrhenius-type viscosity, electrical conductivity, and thermal conductivity models found in literature.

Composition

The general composition range for ferrochrome slag by mass percentage is presented in Table 1.

Table 1. Ferrochrome slag composition range (Das et al. *2023; Geldenhuys 2013*

Slag System	SiO_2	Al_2O_3	FeO	MgO	CaO	Cr_2O_3
Ferrochrome	27-60%	8-38%	1-10%	6-43%	1-23%	2-15%

Structure

Based on the chosen ferrochrome slag composition range, the slag structure is predominantly a three-dimensional silicate network with different fractions of silicate structures (Q^0, Q^1, Q^2, Q^3, Q^4). The Cr_2O_3 content acts as a network breaker. It depolymerises the silicate network, breaking Si-O-Si bonds (lowering Q^3 and Q^4), by dissociating O^{2-} that connects SiO_4^{4-} to other tetrahedrons, into simpler silicon-oxygen tetrahedral structures of chains, layers, and rings. This consequently increases Q^0, Q^1, Q^2 and results in a depolymerised network structure and a reduced viscosity (Wang *et al*., 2023; Nakamoto *et al*; Forsbacka *et al*., 2009).

Viscosity

Studies on ferrochrome slag viscosity have been hampered due to the difficulties in measuring the property. Forsbacka *et al*., (2009) explains that the high melting temperature of chromium-containing slags (T >1400 K) often exceeds the maximum long-term operational range of experimental furnaces and the thermal limits of available construction materials for crucibles and rotating cylinders. Therefore, performing viscosity measurements on ferrochrome slags is expensive as the high-temperature refractory materials can often only be used once or for a limited time. Conducting the measurements is also time-consuming due to the long furnace heating and cooling times, along with sample preparation

and analysis. The experimental runs can often fail with results from successful runs being subject to large errors (Forsbacka *et al*., 2009).

Another reason is that the slags contain chromium in two oxidation states (Cr^{2+} and Cr^{3+}), which affect viscosity to different degrees. The chromium oxidation state depends on the local oxygen partial pressure, temperature as well as slag composition. Both chromium oxides decrease the slag viscosity but Cr_2O_3 raises slag liquidus temperature and thus limits the measuring range. Therefore, the distribution of the oxides is dependent on measurement conditions, which, consequently, have to be carefully fixed (Forsbacka *et al*., 2007).

The models employed to describe ferrochrome slag viscosity are the Iida, modified Iida, Urbain and modified Urbain models (Forsbacka *et al*., 2007; Wang *et al*., 2023). These models are used to describe various multi-component (Al_2O_3–CaO–CrO–Cr_2O_3–FeO–MgO–SiO_2) slag systems containing CrO and Cr_2O_3 (Forsbacka *et al*., 2009). For in-depth descriptions of these models the referenced literature should be consulted (Forsbacka *et al*., 2007; Wang *et al*., 2023).

Forsbacka *et al*., (2009) reported that the modified Urbain model and modified Iida model models gave reasonable results and confirmed the basic network modifying character of both CrO and Cr_2O_3 with CrO had a slightly stronger basic effect. The modified Urbain model produced estimations that were within 21% error relative to experimental results for the investigated chromium containing slags, and provides a satisfactory level of the average model uncertainty (Forsbacka *et al*., 2007).

Recently, the Urbain model was employed by Wang *et al*., (2023) to investigate the CaO–MgO–Al_2O_3–SiO_2– Cr_2O_3 system. The model parameters were optimised and the study showed that when Cr_2O_3 the mass fraction is in the range of 0.85 % to 2.05 %, the slag viscosity for the system decreases with the increase of Cr_2O_3 content. An average relative error of less than 20% between the experimental viscosity values and the calculated viscosity values was obtained with the optimised Urbain model.

Lastly, a brief mention has to be made of the work of Nakamoto *et al*., (2007) that used a neural network model to investigate the ferrochrome slags viscosity. The results produced from the model estimated that the chromium oxides in ferrochrome slag lowered its viscosity and that the effect of CrO on the viscosity decrease is greater than that of Cr_2O_3 (Nakamoto *et al*., 2007).

Electrical Conductivity

The last reported work found in literature on ferrochrome slags electrical conductivity was the review study by Holappa and Xiao, (2004). The study referenced back to gathered material property information for ferrochrome slag systems (Al_2O_3–MgO–SiO_2–Cr_2O_3) in the Allibert and Verein Deutscher Eisenhüttenleute (1995). The conclusion was made that in general, electrical conductivity decreases with increasing temperature and the effect of oxide seems to be complex, showing a slight maximum in some of the systems with the different chromium oxidation states further complicating the phenomenon. It is also mentioned that due to the technical difficulties in high-temperature measurement and the high melting points of ferrochrome slags the electrical conductivity in these slags is not studied systematically. Further research in this field is required (Holappa and Xiao, 2004).

With the limited information on electrical conductivity and with Cr_2O_3 and FeO always being in low concentration relative to other the base components of ferrochrome slag, the systems of SiO_2–Al_2O_3–MgO–CaO or of SiO_2–Al_2O_3–MgO–CaO–FeO should be used for initial estimations.

For the system, the models of Zhang and Chou, (2010) can be used. Based on the Arrhenius equation, Equation 4, Zhang and Chou (2010) developed a semi-empirical model that factors in the effects of structure and cation size through corrected optical basicity (Λ^{corr}). The parameter B, Equation 23, describing the activation energy is calculated with the Λ^{corr} and best-fit values of m and n for CaO–MgO–Al_2O_3–SiO_2 and CaO–Al_2O_3–SiO_2 slag systems. The values required for calculating σ, from Equation 23, can be found in Table 2. The σ can be calculated for slags with compositions within the range of Λ^{corr} being between 0.58 and 0.67. Particulars of calculating Λ^{corr} should be viewed at the reference (Zhang and Chou, 2010).

$$B = m(\Lambda^{\text{corr}}) + n \quad [23]$$

Table 2. Parameter values for slag systems

System	A ($\Omega^{-1}\text{cm}^{-1}$)	m (J mol^{-1})	n (J mol^{-1})
CaO–MgO–Al_2O_3–SiO_2	5054	323.789	-276.838
CaO–Al_2O_3–SiO_2	9462	319.686	-248.952

The approach used by Zhang *et al.*, (2011) to express σ in terms of μ, Equation 24, can also be applied to CaO–MgO–Al_2O_3–SiO_2 and CaO–Al_2O_3–SiO_2 slag systems with $\ln\mu$ calculated either with the mentioned Riboud, Iida, or Urbain models.

$$\ln\sigma = \frac{(-0.08 - \ln\mu)}{1.18} \quad [24]$$

Lastly, it has to be said, the linear regression model developed by Hundermark, (2003) to describe the electrical conductivity of MgO–CaO–Al_2O_3–SiO_2–FeO slags, Equation 25, as a function of composition may also be an applicable model to estimate σ for ferrochrome slag. It applies from 1623 K to 2023 K.

$$\begin{aligned}\ln\sigma = &\left(19.9 - \frac{47348}{T}\right)X_{Al_2O_3} + \left(15.4 - \frac{24087}{T}\right)X_{CaO} + \left(9.2 - \frac{14151}{T}\right)X_{MgO} \\ &+ \left(-0.5 - \frac{7478}{T}\right)X_{SiO_2} + \left(10.0 - \frac{9140}{T}\right)X_{FeO}\cdot Y_{Fe^{2+}} + \left(65.4 - \frac{82447}{T}\right)X_{FeO}^2\cdot Y_{Fe^{2+}}\cdot Y_{Fe^{3+}} \\ &+ \left(-2.6 + \frac{6642}{T}\right)X_{FeO}\cdot Y_{Fe^{3+}}\end{aligned} \quad [25]$$

Thermal Conductivity

There was unfortunately no literature found specifucally on ferrochrome slag thermal conductivity. The Slag Atlas is also data-deficient in this regard (Allibert and Verein Deutscher Eisenhüttenleute, 1995). This presents a large gap in literature and is an area that requires further research.

As with the limited information on electrical conductivity and Cr_2O_3 and FeO always being in low concentration, simpler systems should then be used for initial estimations. The models by Mills (2011) reporting on the ideal silicate slag compositions such as CaO–Al_2O_3–SiO_2 is the best current option. Equation 26 is applicable at T_{liquid} with κ_{liquid} and μ_{liquid}.

$$\ln\kappa_{\text{liquid}} = -2.178 + 0.282\ln\mu_{\text{liquid}} \quad [26]$$

Relation to Q and $\ln\mu_{\text{liquid}}$

Values obtained from Equations 27 and 28 are applicable only for $2 < Q < 3.2$. Caution should be applied for slags with $Q > 3.2$ and high- Al_2O_3 slags, as it may also have a high CaO content, causing the slag to mainly consist of calcium aluminates and show low μ_{liquid} and κ_{liquid} values (Mills *et al.*, 2011).

$$\mu_{\text{liquid}} = 0.165\exp\left(\frac{Q}{0.817}\right) \quad [27]$$

$$\ln\kappa_{\text{liquid}} = -1.8755 - 0.0893\left(\ln\mu_{\text{liquid}}\right) + 0.0352\left(\ln\mu_{\text{liquid}}\right)^2 \quad [28]$$

Relation with Q

Values obtained from Equation 29 are applicable only for $2 < Q < 3.2$.

$$\ln\kappa_{\text{liquid}} = -1.914 + 0.00037\exp\left(\frac{Q}{0.402}\right) \quad [29]$$

Slag Physical Property Data

In the previous sections literature was reviewed for property models based on structural parameters for high- TiO_2 and ferrochrome slag to determine μ, σ and κ values. However, relevant data sources were not mentioned. Table 3 provides a summary of each slag's system properties and relevant references for associated data. All the reported references are post-publication of the Slag Atlas (Allibert and Verein Deutscher Eisenhüttenleute, 1995).

Table 3. Properties of discussed slag systems and relevant references for data

System	Property	Available data format	References
High-slag	μ	Plotted data	(Hu *et al*., 2018)
		Plotted data	(Hu *et al*., 2021)
		Plotted data	(Kim and Park, 2019)
	σ	Plotted data	(Yan et al., 2021)
		Plotted data	(Hu *et al*., 2019)
		Plotted data	(Kotzé, 2020)
	κ	Plotted data	(Heimo *et al*., 2019)
		Estimated plots, no experimental data	(Kotzé, 2020)
		Plotted data	(Ok et al., 2018)
Ferrochrome slag	μ	Plotted and tabulated data	(Forsbacka *et al*., 2007)
		Plotted and tabulated data	(Forsbacka *et al*., 2009)
		Plotted data	(Nakamoto *et al*., 2007)
		Plotted data	(Sariev *et al*., 2020)
		Plotted data	(Wang *et al*., 2023)
	σ	Plotted and tabulated data	(Zhang and Chou, 2010)
		Plotted data	(Zhang *et al*., 2011)
		Plotted and tabulated data	(Hundermark, 2003)
	κ	Plotted and tabulated data	(Mills, 2011)
		Plotted data	(Mills, Yuan, and Jones, 2011)

CONCLUSION

Literature on the structure, μ, σ and κ of high-TiO_2 and ferrochrome slag was reviewed to provide updated information on physical property models and data. The composition and structure of each slag system were defined and various models based on Arrhenius-type relations described for each property and slag. For both slag systems viscosity was the best described property. Electrical and thermal conductivity models for both slag systems were limited and present an area that requires further research and development. Models based on silicate systems such as SiO_2–Al_2O_3–MgO–CaO were described for use as initial estimates of electrical and thermal conductivity for ferrochrome slags due to the very limited literature found on models for these properties. The work presented in this review is the first iteration with more updated reviews to follow. The plan is to increase awareness of the importance of slag physical property models to industry and to provide the community with more up-to-date resources for calculating these properties as part of practical applications.

NOMENCLATURE

Property	Quantity	Description
Slag Structure	NBO	non-bridging oxygen (mol mol^{-1})
	BO	bridging oxygen (mol mol^{-1})
	NBO/T	non-bridging oxygen to tetragonal ion ratio (mol mol^{-1})
	Q	measure for degree of slag polymerisation
	Λ	optical basicity (mol mol^{-1})
	Λ^{corr}	corrected optical basicity (mol mol^{-1})
Viscosity	μ	viscosity (Pa s)
	k	reaction rate constant (s^{-1})
	A	pre-exponential factor (Pa s)
	B	fitting parameter (Pa s K)
	C	fitting parameter (K)
	E_a	activation energy (J mol^{-1})
Electrical Conductivity	σ	electrical conductivity (S m^{-1} or Ω m^{-1})
	σ_{ionic}	ionic conduction (S m^{-1})
	$\sigma_{\mathrm{ionic,i}}$	ionic conduction of species i (S m^{-1})
	$\sigma_{\mathrm{electronic}}$	electronic conduction (S m^{-1})
	ρ	electrical resistivity (Ω m)
	R	electrical resistance (Ω)
	A_{cross}	cross-sectional area (m^2)
	l	distance current travels (m)
	c_{i}	concentration of species i as a charge carrier (mol m^{-3})
	n_{i}	stoichiometric number of cations in oxide i
	X_{i}	mole fraction of i oxide in slag (mol mol^{-1})
	Y_{i}	mole fraction of transition metal i in oxide (mol mol^{-1})
	z_{i}	charge of species i (C)
	D_{i}	mass diffusion coefficient of species i (m^2 s^{-1})
	μ_{i}	mobility of species i as a charge carrier (m^2 V^{-1} s^{-1})
	V_{m}	molar volume of slag (m^3 mol^{-1})
	β	electronic polarisability (Å^3)
	b	Constant
	m	temperature-dependent constant
	R_{valency}	temperature dependent valency ratio (mol mol^{-1})
Thermal Conductivity	T_{liquid}	liquidus temperature (K)
	κ	thermal conductivity (W m^{-1} K^{-1})
	κ_{liquid}	thermal conductivity at liquidus temperature (W m^{-1} K^{-1})
	κ_{298}	thermal conductivity at 298 K (W m^{-1} K^{-1})

Continued on next page

	κ_{phonon}	phonon thermal conduction (W m^{-1} K^{-1})
	$\kappa_{\mathrm{radiative}}$	radiative thermal conduction (W m^{-1} K^{-1})
	$\kappa_{\mathrm{electronic}}$	electronic thermal conduction (W m^{-1} K^{-1})

Property	Quantity	Description
	$Q_{\text{heat flux}}$	heat flux (W m^{-2})
	ϵ	emissivity
	α	thermal diffusivity (m^2 s^{-1})
	C_p	heat capacity (J mol^{-1} K^{-1})
	ρ	density (g cm^{-3})
	τ	optical density
	a	absorption coefficient (m^{-1})
	d	thickness of sample (m)
	n	refractive index
	v	velocity of phonons through slag (m s^{-1})
	l	mean free path for phonons through slag (m)
	L	Lorenz number (W Ω K^{-2})
Property Constants	F	Faraday's constant (C m^{-1})
	R	gas constant (R = 8.314 J mol^{-1} K^{-1})
	σ	Stefan-Boltzmann constant ($\sigma = 5.67 \times 10^{-8}$ W m^{-2} K^4)

REFERENCES

Allibert, M., and Verein Deutscher Eisenhüttenleute. 1995. *Slag Atlas*. 2nd ed. Düsseldorf: Verlag Stahleisen.

Bockris, J. O'M., J. A. Kitchener, S. Ignatowicz, and J. W. Tomlinson. 1952a. "Electric Conductance in Liquid Silicates." *Transactions of the Faraday Society* 48: 75. https://doi.org/10.1039/tf9524800075.

Bockris, J. O'M, J. A. Kitchener, and A. E. Davies. 1952b. "Electric Transport in Liquid Silicates." *Transactions of the Faraday Society* 48 (0): 536–48. https://doi.org/10.1039/TF9524800536.

Das, Shaswat Kumar, Ankit Kumar Tripathi, Sapan Kumar Kandi, Syed Mohammed Mustakim, Bhagyadhar Bhoi, and Priyanka Rajput. 2023. "Ferrochrome Slag: A Critical Review of Its Properties, Environmental Issues and Sustainable Utilization." *Journal of Environmental Management* 326 (January): 116674. https://doi.org/10.1016/j.jenvman.2022.116674.

Desrosiers, R., F. Ajersch, and A. Grau. 1980. "Electrical Conductivity of Industrial Slags of High Titania Content." In *Preprints [of the] International Symposium on Metallurgical Slags*. Halifax, Nova Scotia: Canadian Institute of Mining and Metallurgy.

Forsbacka, Lasse, Lauri Holappa, Alex Kondratiev, and Evgueni Jak. 2007. "Experimental Study and Modelling of Viscosity of Chromium Containing Slags." *Steel Research International* 78 (9): 676–84. https://doi.org/10.1002/srin.200706269.

———. 2009. "Experimental Study and Modelling of Viscosity of Chromium Containing Slags." In *Proceedings of the VIII International Conference on Molten Slags, Fluxes and Salts*. Santiago: GECAMIN. https://www.pyro.co.za/MoltenSlags2009/0215-Holappa.pdf.

Gan, Lei, Chaobin Lai, and Huihui Xiong. 2016. "Non-Arrhenius Viscosity Models for Molten Silicate Slags with Constant Pre-Exponential Parameter: A Comparison to Arrhenius Model." *High Temperature Materials and Processes* 35 (3): 261–67. https://doi.org/10.1515/htmp-2014-0197.

Geldenhuys, I. J. 2013. "Aspects of Dc Chromite Smelting at Mintek-an Overview." In *Proceedings of INFACON XIII: The Thirteenth International Ferroalloys Congress*, 14. Almaty, Kazakhstan: P. Dipner.

Handfield, G., and G. G. Charette. 1971. "Viscosity and Structure of Industrial High TiO2 Slags." *Canadian Metallurgical Quarterly* 10 (3): 235–43. https://doi.org/10.1179/cmq.1971.10.3.235.

Heimo, Juhani, Ari Jokilaakso, Marko Kekkonen, Merete Tangstad, and Anne Støre. 2019. "Thermal Conductivity of Titanium Slags." *Metallurgical Research & Technology* 116 (6): 635. https://doi.org/10.1051/metal/2019064.

Holappa, Lauri, and Yanping Xiao. 2004. "Slags in Ferroalloys Production - Review of Present Knowledge." *Journal of The South African Institute of Mining and Metallurgy* 104 (August): 429–37.

Hu, Kai, Xuewei Lv, Shengping Li, Wei Lv, Bing Song, and Kexi Han. 2018. "Viscosity of TiO2-FeO-Ti2O3-SiO2-MgO-CaO-Al2O3 for High-Titania Slag Smelting Process." *Metallurgical and Materials Transactions B* 49 (4): 1963–73. https://doi.org/10.1007/s11663-018-1284-x.

Hu, Kai, Xuewei Lv, Wenzhou Yu, Zhiming Yan, Wei Lv, and Shengping Li. 2019. "Electric Conductivity of TiO2-Ti2O3-FeO-CaO-SiO2-MgO-Al2O3 for High-Titania Slag Smelting Process." *Metallurgical and Materials Transactions B* 50 (September). https://doi.org/10.1007/s11663-019-01702-0.

Hu, Kai, Kai Tang, Xuewei Lv, Jafar Safarian, Zhiming Yan, and Bing Song. 2021. "Modeling Viscosity of High Titania Slag." *Metallurgical and Materials Transactions B* 52 (1): 245–54. https://doi.org/10.1007/s11663-020-02002-8.

Hundermark, Rodney. 2003. "The Electrical Conductivity of Melter Type Slags." Master of Engineering, MEng, Cape Town, South Africa: University of Cape Town. http://hdl.handle.net/11427/5316.

Kim, Youngjae, and Hyunsik Park. 2019. "Estimation of TiO2-FeO-Na2O Slag Viscosity Through Molecular Dynamics Simulations for an Energy Efficient Ilmenite Smelting Process." *Scientific Reports* 9 (1, 1): 17338. https://doi.org/10.1038/s41598-019-53961-1.

Kotzé, H. 2020. "A Literature Review and Interpretation of the Properties of High-TiO2 Slags." *Journal of the Southern African Institute of Mining and Metallurgy* 120 (2). https://doi.org/10.17159/2411-9717/894/2020.

Liu, Jun-Hao, G.-H. Zhang, and Kuo-Chih Chou. 2014. "Study on Electrical Conductivities of CaO-SiO2-Al2O3 Slags." *Canadian Metallurgical Quarterly* 54 (2): 170–76. https://doi.org/10.1179/1879139514Y.0000000174.

Liu, Jun-Hao, Guo-Hua Zhang, and Zhi Wang. 2017. "Experimental Study on Electrical Conductivity of MnO-CaO-SiO2 Slags at 1723 K to 1823 K (1450 °C to 1550 °C) and Various Oxygen Potentials." *Metallurgical and Materials Transactions B* 48 (6): 3359–63. https://doi.org/10.1007/s11663-017-1072-z.

Liu, Jun-Hao, Guo-Hua Zhang, Yue-Dong Wu, and Kuo-Chih Chou. 2016. "Electrical Conductivity and Electronic/Ionic Properties of TiO x -CaO-SiO2 Slags at Various Oxygen Potentials and Temperatures." *Metallurgical and Materials Transactions B* 47 (1): 798–803. https://doi.org/10.1007/s11663-015-0499-3.

Liu, Yan-Xiang, Jun-Hao Liu, Guo-Hua Zhang, Jian-Liang Zhang, and Kuo-Chih Chou. 2018. "Experimental Study on Electrical Conductivity of FexO-CaO-SiO2-Al2O3 System at Various Oxygen Potentials." *High Temperature Materials and Processes* 37 (2): 121–25. https://doi.org/10.1515/htmp-2016-0102.

Mills, K. C., and M. Susa. 1992. "Thermal Conductivities of Slags." Report/Guide. Teddington. April 1992. https://eprintspublications.npl.co.uk/1170/.

Mills, K. C., L. Yuan, and R. T. Jones. 2011. "Estimating the Physical Properties of Slags." *Journal of the Southern African Institute of Mining and Metallurgy* 111: 649–58. http://www.scielo.org.za/pdf/jsaimm/v111n10/v111n10a02.pdf.

Mills, Ken. 2011. "The Estimation of Slag Properties." pyrometallurgy.co.za. https://www.pyrometallurgy.co.za/KenMills/index.html.

Mills, Kenneth, Lang Yuan, Zushu Li, and Guohua Zhang. 2013. "Estimating Viscosities, Electrical & Thermal Conductivities of Slags." *High Temperatures - High Pressures* 42 (January): 237–56.

Mills, Ken, Lang Yuan, Zushu Li, Guo Hui Zhang, and Kuo-Chih Chou. 2012. "A Review of the Factors Affecting the Thermophysical Properties of Silicate Slags." *High Temperature Materials and Processes* 31 (November). https://doi.org/10.1515/htmp-2012-0097.

Mott, N. F. 1968. "Conduction in Glasses Containing Transition Metal Ions." *Journal of Non-Crystalline Solids* 1 (1): 1–17. https://doi.org/10.1016/0022-3093(68)90002-1.

Mysen, Bjorn, and Pascal Richet. 2019. *Silicate Glasses and Melts - 2nd Edition*. 2nd ed. Elsevier. https://shop.elsevier.com/books/silicate-glasses-and-melts/mysen/978-0-444-63708-6.

Nakamoto, Masashi, Lasse Forsbacka, and Lauri Holappa. 2007. "Assesment of Viscosity of Slags in Ferrochromium Process." In *11th International Ferroalloys Congress INFACON XI, New Delhi, India, February 18-21, 2007*, 159–64. https://research.aalto.fi/en/publications/assesment-of-viscosity-of-slags-in-ferrochromium-process.

Nakamoto, Masashi, Yoshitugu Miyabayashi, Lauri Holappa, and Toshihiro Tanaka. 2007. "A Model for Estimating Viscosities of Aluminosilicate Melts Containing Alkali Oxides." *ISIJ International* 47 (10): 1409–15. https://doi.org/10.2355/isijinternational.47.1409.

Ok, Kyung Min, Yuji Ohishi, Hiroaki Muta, Ken Kurosaki, and Shinsuke Yamanaka. 2018. "Effect of Point and Planar Defects on Thermal Conductivity of TiO2-x." *Journal of the American Ceramic Society* 101 (1): 334–46. https://doi.org/10.1111/jace.15171.

Pesl, J., and Rauf, H.E. 1999. "High-Temperature Phase Relations and Thermodynamics in the Iron-Titanium-Oxygen System." *Metallurgical and Materials Transactions B* 30 (4): 695–705. https://doi.org/10.1007/s11663-999-0031-8.

Pistorius, P. C. 2008. "Ilmenite Smelting: The Basics." *Journal of the Southern African Institute of Mining and Metallurgy* 108 (January): 35–43. https://www.saimm.co.za/Journal/v108n01p035.pdf.

Sariev, O., S. Kim, Ye Zhumagaliev, B. Kelamanov, M. Sultanov, and N. Nurgali. 2020. "Viscosity and Crystallization Temperature of Ferroalloy Slags from Kazakhstan Ore." *Metalurgija* 59 (4): 525–28. https://hrcak.srce.hr/241209.

Seetharaman, Seshadri, Kusuhiro Mukai, and Du Sichen. 2004. "Viscosities of Slags - an Overview." In *VII International Conference on Molten Slags, Fluxes & Salts*, edited by Fluxes & Salts International Conference on Molten Slags, 31–42. Symposium Series S36 / The South African Institute of Mining and Metallurgy. Cape Town, South Africa: The South African Institute of Mining and Metallurgy.

Thibodeau, Eric. 2016. "A Structural Electrical Conductivity Model for Oxide Melts." *METALLURGICAL AND MATERIALS TRANSACTIONS B* 47 (February): 355–83.

Thibodeau, Eric, Aimen E. Gheribi, and In-Ho Jung. 2016. "A Structural Molar Volume Model for Oxide Melts Part I: Li2O-Na2O-K2O-MgO-CaO-MnO-PbO-Al2O3-SiO2 Melts - Binary Systems." *Metallurgical and Materials Transactions B* 47 (2): 1147–64. https://doi.org/10.1007/s11663-015-0548-y.

Wang, Yifan, Yici Wang, Yunhao Zhang, Yifan Chai, Fengguang Zhao, and Guoping Luo. 2023. "Effect of Cr2O3 on the Viscosity and Structure of Slag (or Glass) of CaO-MgO-Al2O3-SiO2 System." *Korean Journal of Chemical Engineering* 40 (7): 1783–91. https://doi.org/10.1007/s11814-023-1432-0.

Yan, Zhi-ming, Xue-wei Lv, and Zu-shu Li. 2021. "Physicochemical Properties and Structure of Titania-Containing Metallurgical Slags: A Review." *Journal of Iron and Steel Research International*, November. https://doi.org/10.1007/s42243-021-00678-z.

Zaaiman, S., H. Muire, and J. H. Zietsman. 2024. "Slag Physical Property Determination: A Review of Experimental and Computational Methods to Determine Structure, μ, σ, and κ." In *Southern African Pyrometallurgy 2024 International Conference, Johannesburg, South Africa, March 12-14, 2024.*

Zhang, Guo-Hua, and Kuo-Chih Chou. 2010. "Simple Method for Estimating the Electrical Conductivity of Oxide Melts with Optical Basicity." *Metallurgical and Materials Transactions B* 41 (1): 131–36. https://doi.org/10.1007/s11663-009-9298-z.

Zhang, Guo-Hua, Bai-Jun Yan, Kuo-Chih Chou, and Fu-Shen Li. 2011. "Relation Between Viscosity and Electrical Conductivity of Silicate Melts." *Metallurgical and Materials Transactions B* 42 (2): 261–64. https://doi.org/10.1007/s11663-011-9484-7.

Zietsman, J. H., and P. C. Pistorius. 2004. "Process Mechanisms in Ilmenite Smelting." *Journal of the Southern African Institute of Mining and Metallurgy*, 653–60. https://www.saimm.co.za/Journal/v104n11p653.pdf.

Hanno Muire

Materials Engineer in Training
Ex Mente Technologies

Hanno Muire is currently pursuing a Master's degree in the Department of Chemical Engineering at the University of Pretoria. With his academic background, he holds both a Bachelor's and an Honours degree in Chemical Engineering from the same institution. His research is centred around the thermochemistry of layered double hydroxides (LDHs), specifically focusing on sustainable synthesis processes. Recently, he contributed to the academic discourse by publishing an article that comprehensively reviews various thermochemical models applied to LDHs. He is employed at Ex Mente Technologies as a materials engineer in training, where he applies his knowledge and skills to research, model, and simulate material properties for pyrometallurgy processes. He is interested in computational modelling, thermochemistry, thermodynamic properties, thermophysical properties, and programming.